remote sensing

MDPI

Article

From Multi-Sensor Survey to a Multi-Scale Geospatial Digital Twin Foundation of a Historic Hill Town: Fiumefreddo Bruzio, Southern Italy

Caterina Balletti, Enrico Breggion *, Andrea Martino, Luisa Berto, Irene Rocca and Diego Alejandro Talledo

Dipartimento di Culture del Progetto, Università Iuav di Venezia, Santa Croce 191, 30135 Venezia, Italy; balletti@iuav.it (C.B.); amartino@iuav.it (A.M.); lberto@iuav.it (L.B.); irocca@iuav.it (I.R.); diego.talledo@iuav.it (D.A.T.)

* Correspondence: ebreggion@iuav.it

Highlights

What are the main findings?

- Integrating UAV and terrestrial photogrammetry, SLAM and static laser scanning produced a common georeferenced framework linking the historic settlement of Fiumefreddo Bruzio to detailed documentation of five heritage buildings.
- The geospatial architecture connects survey products, building records and seismic assessments across urban, building and macroelement scales, preserving data provenance and distinguishing measured geometry from structural interpretation.

What are the implications of the main findings?

- The workflow provides a transferable foundation for heritage digital twins, with repeated observations and controlled model updates required to progress towards an operational monitoring system.
- Linking building vulnerability to the geospatial dataset helps guide conservation and mitigation priorities.

Abstract

Historic hill towns require geometric information capable of relating urban morphology, construction features, and structural details within a common spatial and semantic framework. This paper presents a multi-sensor, multi-scale geomatics workflow for establishing an integrated geospatial information framework for the historic centre of Fiumefreddo Bruzio in Calabria, southern Italy. A control network of 38 points provided the spatial reference for UAV and terrestrial photogrammetry, six SLAM trajectories, and 270 static laser scans covering five buildings. Point clouds generated by Structure from Motion and range-based sensors were co-registered in the RDN2008/UTM zone 33N coordinate reference system and used to produce orthophotos, digital terrain and surface models, contour lines, textured meshes, and building-scale drawings. These products were organised within an interoperable geospatial information system based on persistent links between settlement-, aggregate-, building-, façade-, space-, and macroelement-level entities. The framework also supported structural characterisation and seismic vulnerability assessment at building and urban scales, linking building screening and potential local mechanisms to their spatial interpretation. The resulting survey-based digital model supports conservation documentation, seismic screening, and street-network analysis, while providing the foundation for future digital twin development rather than

Academic Editor: Deodato Tapete

Received: 18 September 2026
Revised: 27 October 2026
Accepted: 1 November 2026
Published: 3 November 2026

Copyright: © 2026 by the authors. Licensee MDPI, Basel, Switzerland. This article is an open access article distributed under the terms and conditions of the Creative Commons Attribution (CC BY) license.

an operational implementation. The study offers a transferable acquisition-to-information workflow, preserving data provenance and metric quality for risk-informed management of historic settlements.

Keywords: digital twin; multi-sensor survey; UAV photogrammetry; terrestrial laser scanning; SLAM; GIS-based cultural heritage documentation; seismic vulnerability; historic settlement

1. Introduction

Historic centres located in seismic areas are simultaneously repositories of architectural heritage, inhabited systems, and emergency environments. Their preservation cannot be reduced to the documentation of isolated monuments: narrow streets, irregular plots, building aggregates, topographic constraints, and successive transformations shape both cultural value and risk. Fiumefreddo Bruzio represents a significant case study. The settlement occupies a hilltop site in Calabria and is characterised by a compact masonry fabric, limited vehicular access, and a seasonal increase in population. A previous study by the research group shows preliminary results of the integration between urban surveying, building census data, structural assessment, and street-network analysis to formulate an interpretative framework of seismic risk [1]. The present contribution builds on and extends that work by focusing more specifically on the geomatics methods and techniques underpinning the overall research framework. Particular attention is given to the construction of a multiscale spatial and geometric information base and to its role in supporting the integration of built-environment knowledge, structural interpretation, and vulnerability assessment. The specific contribution of the present paper is the detailed documentation of the multi-sensor acquisition and processing workflow, its metric assessment, and the organisation of the resulting information across spatial scales. Previously published building-scale seismic screening results [1] are used to illustrate the integration of structural information within this framework.

The distinction between digital models, digital shadows, and digital twins depends on the degree of automated information exchange with the physical asset [2–4]. A digital model does not involve automatic synchronisation, whereas a digital shadow incorporates automated unidirectional data transfer and an operational digital twin requires bidirectional information exchange. In this study, the term digital twin foundation refers to the structured geometric and geospatial information base developed to support future digital twin implementations, rather than to an operational system.

This distinction is particularly important for cultural heritage. Heritage digital twins have been proposed as environments capable of linking survey data, historical sources, conservation records, interventions, and simulations [5–7]. Research on structural digital twins also shows that observed data can be used to update mechanical models and support reliability condition assessment, while reduced models may be required when high fidelity analyses are computationally too demanding [8]. In historic centres predominantly composed of masonry buildings, this integration is especially relevant because surveyed geometry can support both the assessment of the structural behaviour of buildings as a whole and the analysis of local mechanisms, while also allowing vulnerability results to be related to their spatial distribution within the urban fabric. From this perspective, the reality-based model is not merely a geometric representation, but an updatable basis through which observations, structural information and results can be related and progressively revised. Reality-based knowledge models further demonstrate that the value of the digital twin lies in the traceable association between geometry and

knowledge at the appropriate level of detail [9].

Historic Building Information Modelling (HBIM) has provided a related pathway from point clouds to parametric and semantically enriched representations [10–12]. However, historic centres at the urban scale reveal the limitations of an approach confined to individual buildings: a single platform must accommodate terrain, streets, parcels, building aggregates, individual buildings, architectural elements, diagnostic observations, and structural results. Research on the integration of HBIM and three-dimensional Geographic Information Systems (3D GIS) addresses this need by enabling multi-scale queries and spatial analyses [13,14]. Urban-scale standards such as CityGML and CityJSON provide useful concepts for identifiers, levels of detail, geometric semantics, and data exchange, but these need to be complemented by heritage-specific entities and information on source provenance [15,16].

The geometric basis of such systems is commonly generated through photogrammetry and laser scanning. Image-based modelling provides dense geometry and radiometric information, while laser scanning offers direct distance measurements and robust surface coverage [17,18]. Unmanned Aerial Vehicle (UAV) surveys extend coverage to roofs, courtyards, and terrain, although their accuracy depends on network geometry, camera calibration, image configuration, and independent control [19,20]. Mobile mapping and Simultaneous Localisation and Mapping (SLAM) enable the rapid acquisition of complex trajectories and occluded streets, although drift and loop-closure effects require explicit validation [21–23]. Recent applications to cultural heritage confirm the advantages of integrating aerial, terrestrial, mobile, and static sensors rather than forcing a single technique to operate across all scales [24–26]. The scientific contribution of this research lies in the development of an integrated multi-sensor and multi-scale geomatics framework capable of providing a metrically controlled and georeferenced representation of a complex historic settlement. While the integration of different surveying technologies is already well established in cultural heritage documentation, the proposed approach focuses on the construction of a coherent geometric information base that preserves the relationships between different spatial scales, the characteristics of the acquired datasets, and their metric reliability. The resulting geomatics framework represents an essential knowledge infrastructure for subsequent applications, including HBIM, 3D GIS, structural assessment, and the future development of digital twins. Rather than implementing these applications as a single comprehensive system, the present study demonstrates how accurate, multi-source geometric documentation can support their development while maintaining the distinction between measured data and subsequent modelling and interpretation.

On this basis, the study pursues three objectives: (i) to formalise the multi-sensor survey of Fiumefreddo Bruzio as a reproducible workflow from data acquisition to final products; (ii) to define a multi-scale geospatial architecture linking reality-based geometry with information on conservation and risk, showing how the same information basis can support structural characterisation, seismic vulnerability assessment, and their interpretation at the urban scale; and (iii) to establish a transparent framework for assessing and validating the maturity of the digital representation, defining the steps through which the current information basis can evolve into an updatable digital shadow and, subsequently, into a monitoring-enabled digital twin. The scientific contribution is therefore primarily methodological, demonstrating how metrically controlled multi-sensor data can be transformed into a traceable, multi-scale geospatial information framework supporting structural interpretation and seismic risk assessment.

Case Study and Digital Twin Requirements

Fiumefreddo Bruzio is located on the Tyrrhenian side of the Calabrian Apennines in southern Italy. The historic centre occupies an elevated site and is structured by a dense network of streets, stepped paths, small squares, and building aggregates that follow the natural slope of the terrain. The urban fabric is predominantly characterised by traditional masonry construction, including irregular stone masonry, vaulted spaces, timber or mixed floor systems, and buildings modified over time through successive additions. Settlement-scale morphology and the construction characteristics of individual building units are therefore closely interconnected, both in terms of documentation and risk assessment.

The survey campaign addressed the entire historic centre at the urban scale and five buildings at a higher level of detail: Castello della Valle, Santa Maria de Andexis, Santa Chiara, San Rocco, and Addolorata. These architectural assets differ in terms of accessibility, size, construction history, and surveying constraints. They also provide a common field of application for geomatics, architectural analysis, structural assessment, and conservation planning. Figure 1 provides an overview of the compact settlement and highlights its steep topography, which represents one of the main factors motivating the adoption of a multi-sensor survey strategy.



Figure 1. View of Fiumefreddo Bruzio and its compact historic urban fabric.

The information requirements were derived from the decisions that the system is intended to support. At the settlement scale, planners need information on terrain and built morphology, street routes, accessible spaces, and the location of strategic buildings. At the building-aggregate and individual-building scales, the required information includes footprints, shared walls, heights, construction typologies, occupancy status, vulnerability indicators, and links to building census records. At the architectural scale, plans, sections, elevations, and the identification of openings, discontinuities, and visible

deterioration become particularly relevant. At the structural scale, macro-elements, masonry connections, cracks, and deformations need to be located and monitored.

A single geometric resolution cannot effectively meet all these requirements. The proposed architecture therefore treats scale as an explicit property of each representation rather than as an implicit zoom level. Urban-scale products are designed for representation at 1:200 scale, whereas the documentation of the main buildings is intended for 1:50 scale. Dense point clouds generated by the different survey techniques remain available as source evidence, while derived products are optimised for specific analytical and communication purposes.

The implemented system integrates georeferenced survey data, three-dimensional representations, architectural information, and structural assessment results within a common geospatial framework. At its current stage, it represents a survey-based digital model, providing the geometric and information basis for future developments involving automated updates and monitoring.

2. Materials and Methods

2.1. Survey Planning and Common Reference System

The survey campaign of the historic centre of Fiumefreddo Bruzio was designed to establish a metrically consistent, multi-scale geometric framework, connecting the urban morphology with the detailed architectural documentation of five selected heritage buildings. The compact configuration of the settlement, its steep topography, narrow streets, complex geometries, and limited accessibility required the integration of complementary surveying techniques.

The three-day campaign combined GNSS surveying, UAV and terrestrial photogrammetry, handheld SLAM mobile mapping, and terrestrial laser scanning (TLS). Each technique contributed geometric information at different spatial scales and levels of detail, overcoming the limitations associated with individual acquisition methods. The specific survey configurations and processing procedures are described in the following sections. A GNSS control network, established using Network Real-Time Kinematic (NRTK) positioning, provided the common spatial reference for the entire survey. The 38 control points were distributed according to the morphology and accessibility of the historic centre and established the common geodetic reference for the survey.

All acquisitions were integrated within the RDN2008/UTM Zone 33N (EPSG:6708) reference system. UAV and terrestrial photogrammetric blocks were oriented using ground control points (GCPs). SLAM datasets were aligned to the same reference system using surveyed control points, whereas TLS scans were first registered into individual building blocks and subsequently georeferenced through rigid transformations.

The geometric consistency between the different datasets was assessed through qualitative comparisons of stable surfaces and corresponding profiles in overlapping areas. This approach ensured a coherent spatial relationship between urban-scale and architectural-scale representations while preserving the specific geometric characteristics and metric reliability of each acquisition technique. The resulting common geodetic framework provides the basis for integrating point clouds, three-dimensional models, orthophotos and architectural drawings into a consistent multi-scale geospatial information system.

2.2. GNSS Control Network

The GNSS control network for the Fiumefreddo Bruzio survey was established using a Stonex S900A receiver operating in NRTK mode and the Hexagon SmartNet differential correction service, with the aim of providing a common metric control framework

for the orientation of the photogrammetric blocks, the georeferencing of the derived products, and the assessment of spatial consistency among UAV, terrestrial photogrammetry, SLAM, and TLS datasets. A total of 38 control points were surveyed across the entire study area and positioned on stable and clearly identifiable surfaces suitable for subsequent recognition in both the photogrammetric datasets and the point clouds.

In the specific case of Fiumefreddo Bruzio, the layout of the GNSS control network was strongly influenced by the site morphology and the compactness of the built fabric. The historic center occupies an elevated area characterized by narrow streets, pronounced elevation changes, continuous walls, internal courtyards, and closely spaced building façades. These conditions reduce sky visibility and may lead to signal masking and multipath effects, particularly along routes within the urban core. For this reason, the control points were not arranged according to a regular grid but were distributed in response to the actual conditions of the settlement: along its perimeter, at open spaces and road junctions, in unobstructed areas close to access points, along the upper and lower edges of the historic center, and at selected internal locations that were sufficiently recognizable in both aerial and terrestrial imagery.

The control network (Figure 2) was conceived to serve a dual purpose. On the one hand, a subset of the points was used as reference for the absolute georeferencing of the datasets, particularly for the UAV photogrammetric block and for the control of the urban-scale survey products. For the UAV photogrammetric blocks, a separate subset was retained as independent check points, allowing coordinate differences to be assessed at points excluded from the adjustment.



Figure 2. The GNSS control points network.

The surveyed points were progressively labelled from CP01 to CP38 and referenced to the Italian national geodetic system RDN2008, using the UTM Zone 33N projection. The same reference system was maintained throughout the entire processing workflow, avoiding undocumented local transformations between the different products. This

choice was essential to ensure spatial consistency among the urban orthophoto, DSM, DTM, meshes, point clouds, cross-sections, elevations, and GIS layers. In particular, the adoption of a single reference system made it possible to treat urban-scale and architectural-scale products as components of the same metric framework, reducing the risk of misalignment among roofs, façades, and the internal geometries of the priority buildings.

The prefix CP in the point identifiers is a field label and does not denote the processing role. GCPs are points used as constraints, whereas independent check points are excluded from the adjustment and from any subsequent transformation or refinement being evaluated. Point roles are dataset-specific; the UAV allocation and the GCPs used for the SLAM acquisitions are reported in the next sections.

For UAV photogrammetry, the control/check configuration reported for both UAV flight blocks comprised 20 GCPs and eight withheld CPs . The six SLAM acquisitions used 4, 4, 9, 4, 7 and 9 GCPs, respectively . These counts refer to the processing role within each dataset.

No separate independent CP set was used for the SLAM or TLS blocks; residuals at their georeferencing points describe fitting quality.

The NRTK measurements provided precision levels suitable for using the surveyed points as control for photogrammetric and laser scanning surveys at both urban and architectural scales. The recorded values of σE, σN, and σH indicate a horizontal precision generally ranging from 1.0 to 1.9 cm and a vertical precision ranging from 1.8 to 3.4 cm. As expected for NRTK measurements performed in a complex urban environment, the vertical component was, on average, less precise than the horizontal components, while remaining fully compatible with the objectives of the survey. The highest precision was observed for points located in more open areas, such as squares, access points, and road edges, whereas slightly higher uncertainty values were found for points located along slopes, vegetated margins, or partially obstructed areas, where satellite geometry and signal stability may be less favorable.

These GNSS precision estimates describe the reference observations and are not equivalent to the accuracy of the derived point clouds. Check-point discrepancies also include reference-coordinate uncertainty; common NRTK systematic effects may remain shared by control and check points.

2.3. UAV Photogrammetry

The aerial photogrammetric survey of the historic center of Fiumefreddo Bruzio was carried out using a DJI Mavic 3 Multispectral UAV equipped with its integrated RGB sensor. The choice of platform was driven by the need to acquire a high-resolution dataset over a compact historic settlement developed on a steep slope and characterized by irregular roofs, closely spaced buildings, streets of varying width, and substantial elevation differences between the upper and lower parts of the town. In this context, nadir imagery alone would not have provided sufficient coverage of roof edges and the most exposed vertical surfaces. For this reason, as previously noted, the UAV survey campaign combined nadir and oblique image acquisition.

The UAV survey was organized into two separate flight blocks (Figure 3), acquired at different altitudes, and designed to fulfill complementary metric objectives. The first block, flown at a lower altitude, focused exclusively on the built-up historic center and was intended to provide detailed documentation of the urban fabric, roofs, squares, open spaces, and the main building edges. The second block, acquired at a higher altitude, covered a wider area, including the surrounding hillside, access routes, adjacent green areas, and the morphological relationships between the historic settlement and the

local topography. This distinction made it possible to obtain two complementary levels of information: a denser dataset suitable for detailed analysis of the built environment and a more extensive dataset supporting the contextualization of the historic center within its immediate territorial setting.

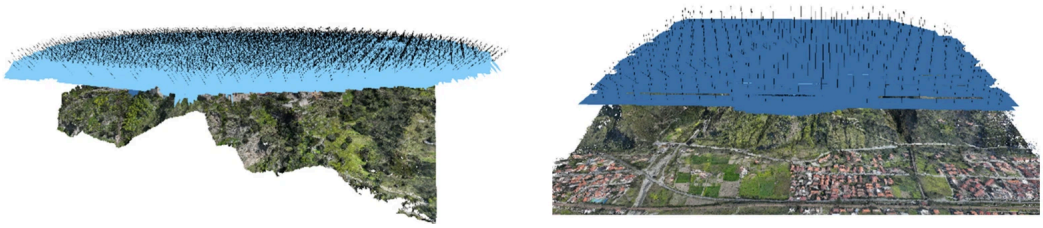


Figure 3. The two photogrammetric flights: the 35 m-altitude plan on the left and the 65–80 m-altitude plan on the right.

The first flight plan over the built-up area was acquired at an average altitude of approximately 35 m above the rooftops, with an estimated Ground Sampling Distance (GSD) of about 2 cm/pixel. This configuration was adopted to preserve a high level of detail over roof surfaces and open spaces within the historic urban fabric. The images were acquired along flight strips with high forward and side overlap and were complemented by oblique imagery aimed at improving the documentation of façades and roof edges. For this block, the adopted overlap was 85% in the flight direction and 75% in the transverse direction, values consistent with the need to ensure sufficient redundancy in an urban environment characterized by pronounced geometric discontinuities.

The second UAV plan was acquired at a higher altitude, approximately 65–80 m above the mean elevation of the survey area, with an estimated GSD ranging from 3.5 to 5 cm/pixel. The purpose of this flight was to extend the coverage beyond the built-up core, including the surrounding hillside, external road network, paths, agricultural surfaces, and sparsely vegetated areas around the settlement. The products derived from this block were used primarily for morphological contextualization, for ensuring continuity of the overall orthophoto, and for generating elevation models at the urban-territorial scale. Compared with the detailed block, the higher-altitude flight prioritized areal continuity and the overall stability of the model, reducing discontinuities along the margins of the historic center.

A total of 8850 RGB images were acquired, including both nadir and oblique views. The nadir images provided the primary dataset for generating the orthophoto, DSM, DTM, and contour lines, whereas the oblique images contributed to improving orientation robustness and the reconstruction of surfaces that could not be adequately observed from above. In the case of Fiumefreddo Bruzio, oblique imagery was particularly important along the margins of the historic center, where the compact built fabric produces shadows, closely spaced vertical façades, and pronounced elevation differences over short distances.

The coordinates of the image projection centers were acquired by the UAV's integrated GNSS system. The latitude, longitude, and ellipsoidal height associated with each image were extracted from the metadata and checked prior to import into the photogrammetric processing software. The projection-center coordinates, originally acquired in the geographic RDN2008 reference system, were converted to the national projected reference system RDN2008/UTM Zone 33N using ConveRgo and the corresponding transformation grids supplied by the Italian Military Geographic Institute (IGM) [27]. This transformation was necessary to ensure consistency among the image projection centers, the ground-surveyed GNSS points, the GIS layers, and the final metric

products.

The conversion of the image projection-center coordinates represented a critical stage of the workflow, since the entire absolute orientation process depended on the consistency between the image coordinates and the reference system of the control points. After conversion, the coordinates were reimported into the photogrammetric project and used as initial observations for image orientation. The reference system adopted for processing was RDN2008/UTM Zone 33N, consistently with the GNSS control network described in the previous section. This constituted the initial direct georeferencing stage, providing a reference for the subsequent refinement with surveyed GCPs and assessment at CPs.

Photogrammetric processing was carried out following a Structure-from-Motion (SfM) workflow. The first stage consisted of image orientation, including the estimation of both interior and exterior orientation parameters. The combined use of nadir and oblique imagery improved the geometry of the photogrammetric block, reducing the limitations typically associated with urban surveys based exclusively on vertical imagery.

After initial image alignment in Agisoft Metashape (version 2.1.1), camera-location residuals were evaluated against the imported coordinates of the image projection centres (Table 1). The table reports the component RMSE values and the three-dimensional "Total error" for this initial georeferencing stage. These residuals describe agreement between estimated and reference camera positions; they do not provide an independent assessment of reconstructed surface accuracy.

Table 1. Coordinate-error summary for the initial direct georeferencing stage.

RMSE E (m)	RMSE N (m)	RMSE H (m)	RMSE 3D (m)
0.032	0.026	0.038	0.056

For both UAV flight blocks, after the initial direct georeferencing, 20 of the surveyed GNSS points were used as GCPs to refine the absolute orientation in RDN2008/UTM Zone 33N, while eight were retained as CPs (Table 2). The CP coordinates were excluded from the adjustment and used to assess the final photogrammetric solution independently of the GCP constraints. This distinction was necessary in the case of Fiumefreddo Bruzio because the compactness of the built-up area, internal elevation differences, shadows cast by building façades, and the presence of marginal areas characterized by less favorable imaging geometry could generate local deformations that would not be immediately detectable from a visual assessment of the orthophoto alone.

The RMSE values reported in Table 2 are lower for the GCPs, which constrained the adjustment, and slightly higher for the CPs, whose coordinates were excluded from it. The GCP residuals describe the fit to the control network, while the CP discrepancies assess the final orientation at the withheld points.

Table 2. RMSE of coordinate residuals at GCPs and coordinate differences at independent CPs for the two UAV flight blocks.

Point Role	N°	RMSE E (m)	RMSE N (m)	RMSE H (m)	RMSE EN (m)	RMSE 3D (m)
GCP	20	0.013	0.014	0.018	0.019	0.026
CP	8	0.019	0.018	0.026	0.026	0.037

Each coordinate RMSE is the square root of the mean squared coordinate discrepancy. Horizontal and three-dimensional RMSE values combine the corresponding component RMSE values in quadrature.

Following image orientation, depth maps and a dense point cloud were generated. The depth maps provided the basis for the production of elevation models and the textured mesh. In particular, the UAV dataset was used to derive a DSM representing the visible surfaces, a DTM obtained by filtering above-ground elements, a georeferenced RGB orthophoto, contour lines, and a textured three-dimensional mesh of the entire historic center and the surrounding hilly area. The products derived from the lower-altitude flight were used for the detailed analysis of roofs and urban spaces, whereas those generated from the higher-altitude flight were used to ensure spatial continuity and provide a broader territorial context.

Terrain classification for DTM generation required particular attention. The historic center is characterized by closely spaced built surfaces, terraces, retaining walls, stepped paths, and discontinuously distributed vegetated areas. Under these conditions, automatic filtering may incorrectly classify low roofs, terraces, or walls as ground or, conversely, remove actual portions of the topographic surface in areas characterized by pronounced discontinuities. For this reason, the DTM should be regarded as a derived product requiring local verification, particularly along the margins of the settlement, along paths, and within terraced areas. By contrast, the DSM preserves the complete information on visible surfaces and is therefore more suitable for the volumetric analysis of the settlement and for assessing the continuity of the roofscape.

The urban orthophoto was generated using the surface model considered most appropriate for accurately representing roofs and open urban spaces. The orthophotos were exported at pixel sizes of 2 cm for the historic core and 5 cm for the surrounding area. Maintaining two separate products avoided generating a single orthophoto that would either be oversampled or, conversely, excessively generalized relative to the level of detail actually acquired in the central areas of the historic settlement.

2.4. Terrestrial Photogrammetry

Terrestrial photogrammetry was used to document building façades, confined spaces, and surfaces that could not be adequately captured by the UAV survey. Images were acquired with a Nikon Z7 full-frame mirrorless camera, equipped with a 20 mm lens and a sensor resolution of 45 MP. Approximately 3500 images were collected. Camera-to-object distances generally ranged from 10 to 20 m but were adjusted according to street width, façade height, and accessibility.

Image sequences were acquired along the façades with sufficient overlap between consecutive photographs. Convergent images were added around corners, portals, towers, overhangs, and recesses, where conventional parallel image sequences would have left gaps in the reconstruction. This acquisition geometry reduced the effects of occlusion and helped connect adjacent façade sections. The images were organized by building and surveyed surface, and were checked for sharpness, exposure, and changes in illumination before Structure-from-Motion processing. The photogrammetric blocks were georeferenced in the common coordinate reference system using identifiable control points and corresponding features shared with the UAV and TLS datasets.

High-resolution orthophotos were produced for the façades along the main route through the historic center and for selected interior surfaces. The frescoes inside Castello della Valle were photographed under controlled lighting to reduce reflections and variations in color and brightness (Figure 4). Orthorectification was carried out by projecting the oriented images onto the corresponding three-dimensional reference surfaces.



Figure 4. Orthophoto of a fresco inside Castello della Valle, prepared for representation at a nominal scale of 1:50.

2.5. Handheld SLAM Mobile Mapping

The SLAM survey of the historic center of Fiumefreddo Bruzio was carried out using a Stonex X120GO handheld scanner, with the aim of complementing the UAV dataset and terrestrial photogrammetry in those parts of the settlement characterized by greater occlusion, limited accessibility, and poor visual continuity. SLAM acquisition was primarily concentrated within the built-up area and along the main peripheral pedestrian routes, where the dense urban fabric, narrow alleys, covered passageways, ramps, stairways, and elevation changes made documentation based exclusively on photographic acquisition or individual static scans inefficient.

Six separate SLAM scans were acquired along trajectories incorporating loops and return segments, each covering a specific portion of the historic settlement (Figure 5). The survey was divided into six separate acquisitions to limit trajectory drift, reduce the length of individual continuous paths, and maintain more effective metric control over each surveyed sector. In a compact and irregular historic urban environment, a single

continuous trajectory would have produced a more extensive dataset but would also have been more susceptible to the progressive accumulation of errors, particularly along sections characterized by few distinctive geometric features or abrupt elevation changes.

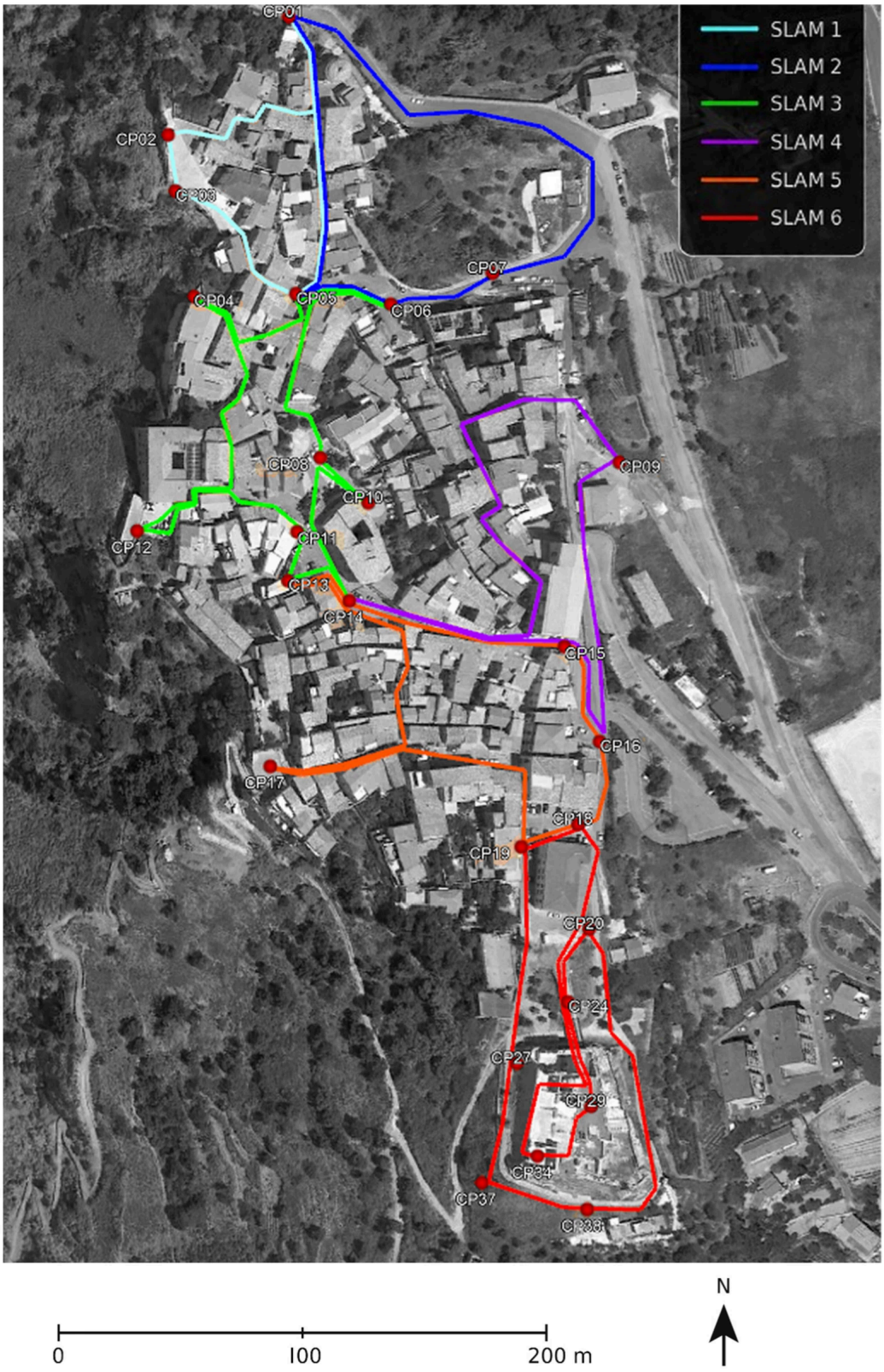


Figure 5. SLAM trajectories.

The trajectories were connected through GNSS-surveyed GCPs shared among ac-

quisitions (Table 3). This configuration made it possible to establish a control chain across the different SLAM blocks, avoiding the treatment of each point cloud as an independent dataset to be subsequently aligned solely through geometric correspondences. The common points were selected among those previously surveyed using GNSS NRTK and were located in open spaces, terraces, small squares, intersections, and paths immediately adjacent to the built-up area. The shared points linked the acquisitions to a common geodetic reference, supporting geometric continuity across neighbouring sectors.

The path of each scan was planned to maintain a regular walking speed while avoiding abrupt rotations of the instrument and prolonged stops in areas affected by moving people, vehicles, or vegetation. Within the historic settlement, the operator prioritized looped trajectories, repeatedly returning to previously acquired open spaces or intersections in order to provide favorable conditions for trajectory closure. Along paths and terraced sections, where complete loops could not always be achieved, partial returns and overlaps with known control points were introduced to limit the propagation of drift.

SLAM acquisition was primarily aimed at ensuring geometric continuity along traversable routes and spaces. Compared with the UAV survey, mobile mapping enabled the documentation of the lower portions of building façades, underpasses, entrance halls, elevation changes, and pedestrian connections that were not always visible from above. Compared with static TLS, SLAM provided faster and more continuous coverage, which was particularly useful for connecting different parts of the historic settlement that could not be observed directly from a single scanning station. For this reason, the SLAM dataset was not considered a replacement for static scanning but rather as an intermediate survey layer between UAV-based urban coverage and the detailed metric survey of the priority buildings.

The orientation of the six scans was carried out in two stages. In the first stage, each trajectory was processed separately, preserving its internal geometry and visually inspecting point-cloud continuity and local misalignments in revisited areas. The software reports did not provide a numerical loop-closure error. In the second stage, the six point clouds were transformed into the common RDN2008/UTM Zone 33N reference system using the GCPs surveyed with GNSS NRTK. The use of shared control points between adjacent scans made it possible to constrain their relative alignment and to verify geometric continuity across the transition areas between neighboring sectors.

The qualitative assessment of the scans was carried out by comparing the SLAM point clouds with the GCPs and with stable surfaces identifiable in the photogrammetric and TLS datasets. The checks focused on paved surfaces, perimeter walls, thresholds, building edges, parapets, terraces, and road sections that remained unchanged during the survey campaign. These features were used to identify any residual rotations, horizontal offsets, vertical discontinuities, or local deformations of the reconstructed trajectories.

The six scans showed residuals consistent with the intended use of SLAM data for ensuring urban-scale continuity and connecting the different datasets. Mean residuals at the GCPs ranged from 2.4 to 3.5 cm in planimetry and from 3.1 to 4.9 cm in elevation, with lower values observed in inner urban areas characterized by abundant vertical geometric features and slightly higher values along vegetated paths and peripheral sections (Table 4). These residuals describe the fit to the GCPs used for georeferencing.

Table 3. Survey configuration of the six SLAM scans and shared GCPs.

Scan	Running Time	Length (m)	Used GCPs
SLAM 1	5′26″	326	CP01, CP02, CP03,

Scan	Running Time	Length (m)	Used GCPs
SLAM 2	7′06″	427	CP05 CP01, CP05, CP06, CP07
SLAM 3	10′05″	605	CP04, CP12, CP11, CP13, CP14, CP10, CP8, CP6, CP5
SLAM 4	8′31″	512	CP14, CP15, CP16, CP9
SLAM 5	8′46″	526	CP13, CP14, CP15, CP16, CP18, CP19, CP17
SLAM 6	10′30″	630	CP18, CP19, CP27, CP37, CP38, CP20, CP29, CP34, CP24

Table 4 reports the mean horizontal distance, mean absolute height difference and maximum three-dimensional distance at the GCPs used to georeference each SLAM acquisition. These statistics describe the georeferencing fit; they do not measure independent accuracy along the trajectories.

Table 4. Georeferencing residuals at the GCPs used for the six SLAM acquisitions.

Scan	GCP (*n*)	Mean Horizontal Residual (m)	Mean Absolute Vertical Residual (m)	Maximum 3D Residual (m)
SLAM 1	4	0.024	0.031	0.047
SLAM 2	4	0.027	0.034	0.052
SLAM 3	9	0.026	0.033	0.050
SLAM 4	4	0.029	0.038	0.058
SLAM 5	7	0.035	0.049	0.071
SLAM 6	9	0.032	0.046	0.068

The main limitation of the SLAM survey concerned the areas outside the compact urban core, particularly the western paths and terraced areas, where vegetation, less regular surfaces, and a lower density of stable vertical features may reduce localization robustness. By contrast, within the narrow streets of the historic center, the presence of continuous façades, building edges, thresholds, and lateral walls contributed to greater geometric stability of the trajectory, although careful handling was still required to limit abrupt rotations of the instrument and sudden elevation changes.

The integrated SLAM point cloud was used to complete the three-dimensional representation of the historic settlement in areas where the UAV dataset was partially occluded and where terrestrial photogrammetry did not provide sufficient spatial continuity. In particular, the dataset supplied useful information for reconstructing pedestrian routes, connections between different elevation levels, the lower portions of building façades, and the links between open spaces and the entrances to the priority buildings. In the case of Fiumefreddo Bruzio, the main contribution of SLAM was therefore to ensure geometric continuity between the urban and architectural scales, rather than to generate standalone final metric products.

The adopted procedure made it possible to integrate the mobile mapping data into

the overall metric framework of the survey without assigning it an inappropriate role as an absolute reference. The GCPs shared between adjacent scans enabled the connections between trajectories to be checked and reduced the risk of local misalignments between neighboring sectors.

2.6. TLS Scans

Terrestrial laser scanning was used for the detailed survey of five buildings: Castello della Valle and the churches of Santa Maria de Andexis, Santa Chiara, San Rocco, and Addolorata. The survey comprised 270 scan positions acquired with a FARO Focus3D S 120 phase-shift scanner. Stations were set up inside the buildings and in the surrounding open spaces. The scanner has a nominal operating range of 0.6–120 m, a maximum measurement rate of 976,000 points/s, and a field of view of 360° horizontally and 305° vertically. The manufacturer reports a ranging error of ±2 mm at 10 m and 25 m. At 10 m, the ranging noise is 0.6 mm on surfaces with 90% reflectivity and 1.2 mm on surfaces with 10% reflectivity [28].

The resolution was set to 1/4 and the quality to 3×. Over the full angular range, this configuration yields approximately 43.7 million points. Laser acquisition took approximately 3 min 45 s per position, increasing to about 6 min when colour-image capture was included. For the complete set of 270 scans, this corresponds to roughly 27 h of acquisition and a theoretical maximum of 11.8 billion raw points. Fieldwork took longer because the estimate does not include positioning and levelling the scanner, moving between stations, checking the acquired data, or storing the files.

The station layout was adapted to the geometry of each building. Fragmented rooms, narrow staircases, changes in level, and irregular connections between spaces often required short distances between consecutive setups. Additional stations were placed near doorways and corridors to maintain overlap and reduce occlusions. The point spacing given above refers to the sampling setting of the scanner. The density of the recorded point cloud is not uniform and varies with range, angle of incidence, surface reflectance, occlusions, missing returns, and filtering.

Data processing was carried out in Leica Cyclone REGISTER 360 (Version 2025.0.1). A separate registration block was created for each building to resolve the relative geometry of rooms and connecting passages before georeferencing. Within these blocks, consecutive scans were aligned by cloud-to-cloud matching in their common areas. Alignment was checked on stable masonry surfaces and on clearly recognisable architectural features visible in neighbouring scans.

Registration quality was summarized using the mean cloud-to-cloud error, overlap and strength reported for the retained scan links, together with visual inspection of stable masonry surfaces and recognizable architectural features (Table 5). These software indicators characterize local registration consistency.

Table 5. TLS registration quality indicators and georeferencing fit statistics for the surveyed sites.

Building	Georef. Points *n*.	Mean C2C (m)	Mean Overlap (%)	Mean Strength (%)	Georef. Fit RMSE 3D (m)
Castello della Valle	5	0.006	58	72	0.028
Santa Maria de Andexis	4	0.005	61	75	0.025
Santa Chiara	4	0.004	64	78	0.023

Building	Georef. Points *n*.	Mean C2C (m)	Mean Overlap (%)	Mean Strength (%)	Georef. Fit RMSE 3D (m)
San Rocco	4	0.007	52	66	0.032
Addolorata	4	0.006	55	69	0.029

After local registration, each building block was georeferenced in the RDN2008/UTM zone 33N coordinate reference system. The georeferencing used corresponding architectural points identified in the TLS clouds, whose reference coordinates were extracted from the already georeferenced photogrammetric and SLAM clouds. This transferred the existing urban reference to the building interiors, where roofs and walls constrain GNSS positioning, while retaining the relative geometry established during local registration. The resulting point clouds could therefore be compared directly with the photogrammetric and SLAM data and related to the roofs, exterior surfaces, and surrounding urban fabric.

For the illustrative configuration in Table 5, five architectural correspondences were used for Castello della Valle and four for each church, with reference coordinates extracted from the existing photogrammetric and SLAM clouds. The georeferencing fit was summarized separately as the RMS three-dimensional distance between the transformed TLS correspondences and their reference positions. Because these correspondences constrained the transformation, their residuals describe fitting quality rather than independent positional accuracy.

The TLS point clouds were the main geometric source for drawing plans, elevations, and sections at a nominal scale of 1:50. They also supported the measurement of wall thicknesses, out-of-plumb walls, geometric irregularities, and discontinuities in the masonry. UAV and terrestrial photogrammetry extended the coverage to the roofs and the wider urban setting and provided complementary radiometric information for the exterior surfaces.

2.7. Point-Cloud Co-Registration and Integration

Point clouds acquired with the different sensors were integrated through a hierarchical workflow, while the sensor-specific datasets were kept separate. The UAV block followed the two-stage georeferencing described in Section 2.3, and the SLAM clouds were georeferenced using the surveyed GCPs. For TLS, local registration within each building was followed by a rigid transformation into the RDN2008/UTM zone 33N coordinate reference system using corresponding points extracted from the photogrammetric and SLAM clouds. This sequence preserved the internal geometry of each TLS block and avoided forcing a non-rigid adjustment between datasets with different resolutions and accuracy levels.

The UAV, terrestrial-photogrammetry, SLAM, and TLS point clouds were compared in their areas of overlap using stable, geometrically recognisable surfaces. In areas characterised by markedly different point densities or measurement accuracies, filtering and decimation parameters were adjusted for each dataset. The purpose was to obtain manageable point clouds while retaining sufficient geometric detail and accuracy for the intended representation scales.

These comparisons were qualitative and assessed consistency within the shared reference framework; they did not provide independent cross-sensor error statistics.

Each derived product retained a link to its source dataset, acquisition sensor and date, coordinate reference system, processing parameters, and available metric checks. Integration was therefore treated as the co-registration of multiresolution survey evi-

dence rather than as the irreversible merging of all observations into a single point cloud with no record of their provenance.

2.8. HBIM Potential Implementation

The proposed information framework adopts a multi-scale geospatial approach in which reality-based geometric representations are associated with architectural, historical, and structural information.

The implemented survey products include georeferenced point clouds, textured meshes, orthophotos, and CAD drawings derived from the integration of photogrammetric and laser scanning datasets, as described in the following Section 4. The GIS component enables these geometric representations to be related to spatial entities representing buildings and their associated information, including construction characteristics and seismic vulnerability assessments.

Although the conceptual framework draws on HBIM principles, particularly the semantic organisation of architectural information and the association between geometry and attributes, the present implementation does not document the creation of a comprehensive parametric HBIM model or a BIM-to-GIS interoperability workflow.

Accordingly, HBIM is considered a potential extension of the proposed geospatial architecture rather than a fully implemented component of the current system. Future developments may introduce parametric representations of selected architectural and structural elements, establishing explicit relationships between HBIM objects and their corresponding GIS entities through persistent identifiers.

2.9. From Multi Scale Survey to Structural Assessment/Interpretation

The multi-scale survey is conceived not only as a geometric documentation layer, but also as a basis for structural analysis. Georeferenced point clouds, textured meshes, orthophotos, and CAD drawings (i.e., plans, sections) provide a detailed representation of the geometry and configuration of the surveyed structures, supporting the identification of the main features that influence their seismic response (e.g., storey heights, wall thicknesses, openings, irregularities, out of plumbness, existing crack patterns, mutual constraints within aggregates). When combined with the building census and with information on construction characteristics and conservation conditions, these data are used for the assessment, connecting the surveyed geometry to the assumptions required for the structural analysis. In this way, the reality-based representation and the engineering interpretation are maintained as interconnected components of the same geospatial framework.

For seismic screening, the previous application to Fiumefreddo Bruzio [1,29] adopted a hybrid quantitative–qualitative procedure to assess the global behaviour of masonry buildings, based on the simplified methodology proposed by Ferretti, et al. [30] . The procedure estimates the building collapse capacity in terms of peak ground acceleration (PGAc), combining an analytical evaluation of the shear capacity of masonry piers with qualitative parameters describing construction quality and structural configuration. The assessment of global response can then be complemented by simplified kinematic analyses aimed at studying possible local out-of-plane mechanisms. To this purpose the identification of structural irregularities, openings, out-of-plumbness, and existing crack patterns are essential. These analyses are particularly relevant in historic masonry structures, where local instability may strongly depend on the geometry of individual portions and on their connections with the surrounding structural system. Moreover, high-resolution survey data provide a valuable basis for refining the analyses of out-of-plane mechanisms exploiting the higher accuracy for the definition of geome-

try and constraints required.

The building collapse capacity is compared with the corresponding seismic demand calculated based on georeferenced position of the building, by means of an ad hoc developed QGIS processing plugin that computes seismic data starting from the MPS04 Seismic hazard grids as adopted by the Italian Building Code [31,32] and the seismic micro zonation dataset [33].

Within the proposed information architecture, the outcomes of structural assessment can be linked to persistent identifiers associated with buildings or individual macroelements, while retaining the information needed to reconstruct the corresponding assessment process. Rather than storing structural results as isolated outputs, the system can therefore relate them to the assumptions, parameters, analysis scenario and model version from which they were obtained. This approach preserves a clear distinction between surveyed information and its structural interpretation and, at the same time, provides a traceable basis for subsequent updates. New inspections, observed damage or repeated surveys can thus be incorporated as additional information and used, where necessary, to revise the structural assessment while preserving previous model states.

3. Results

3.1. Urban Scale Products

As introduced in the previous sections, the UAV photogrammetric block covering the historic settlement produced an RGB orthophoto with a GSD of 2 cm, while the larger-area block generated an orthophoto with a resolution of 5 cm/pixel (Figure 6). The two products address complementary needs: the former provides a high level of detail for the historic core, whereas the latter ensures spatial continuity with the surrounding slope, access roads, and adjacent areas. Within the GIS platform, the orthophotos provide a reference base for verifying building footprints, spatially linking building census records, and updating and integrating the street-network graph using the data already available from OpenStreetMap. Information on the road network was further enriched by recording the width of streets and paths, identifying potential points of interest, and classifying individual segments according to accessibility and use, distinguishing between pedestrian streets, pedestrian streets accessible by residents' vehicles only, driveways, and unpaved tracks.



Figure 6. RGB orthophoto of the historic centre and its immediate surroundings, with a ground sampling distance (GSD) of 5 cm.

The DSM provides a continuous representation of the surveyed surfaces, including buildings, vegetation, and other above-ground elements, whereas the DTM, derived from the classification of ground points, describes terrain morphology, elevation patterns, and associated slopes (Figure 7). In areas characterised by retaining walls, terraces, low roofs, and narrow streets, point classification required local verification and correction, as filtering errors may affect the accurate representation of elevations, slopes, and, consequently, contour lines.

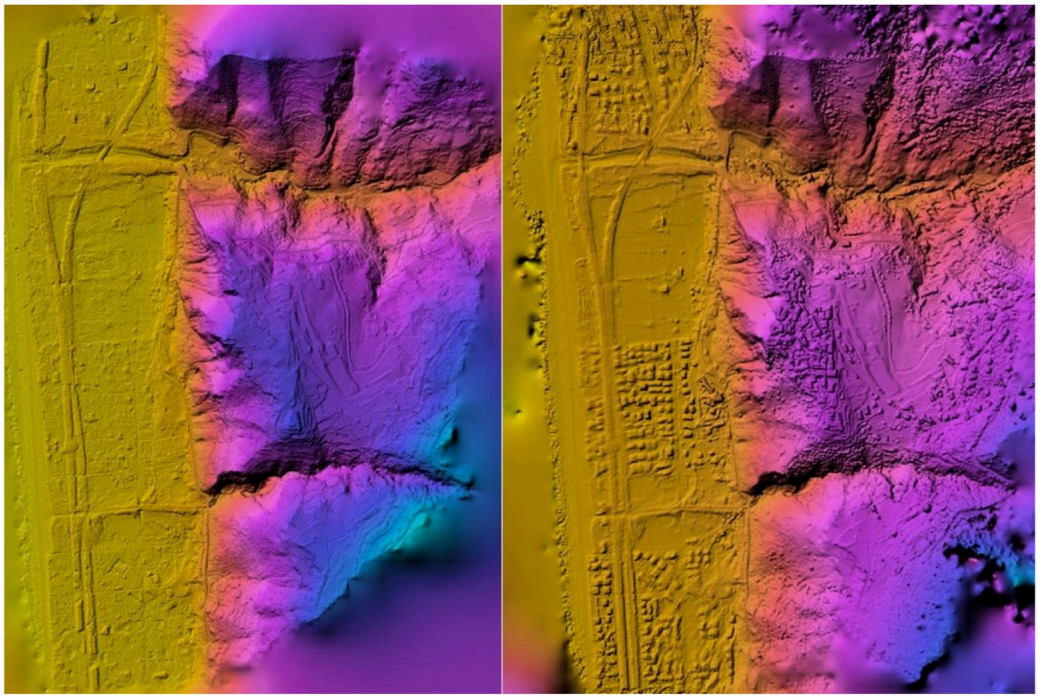


Figure 7. Digital terrain model (**left**) and digital surface model (**right**).

An additional product is the textured mesh (Figure 8), which provides a continuous representation of the three-dimensional morphology of the historic settlement, the relationships between roofs, buildings, and terrain, and the overall volumetric articulation of the urban fabric. Starting from the high-resolution mesh, a lightweight version of the model was also generated through decimation, reducing the geometric complexity and optimising the dataset for web-based visualisation and interactive access.

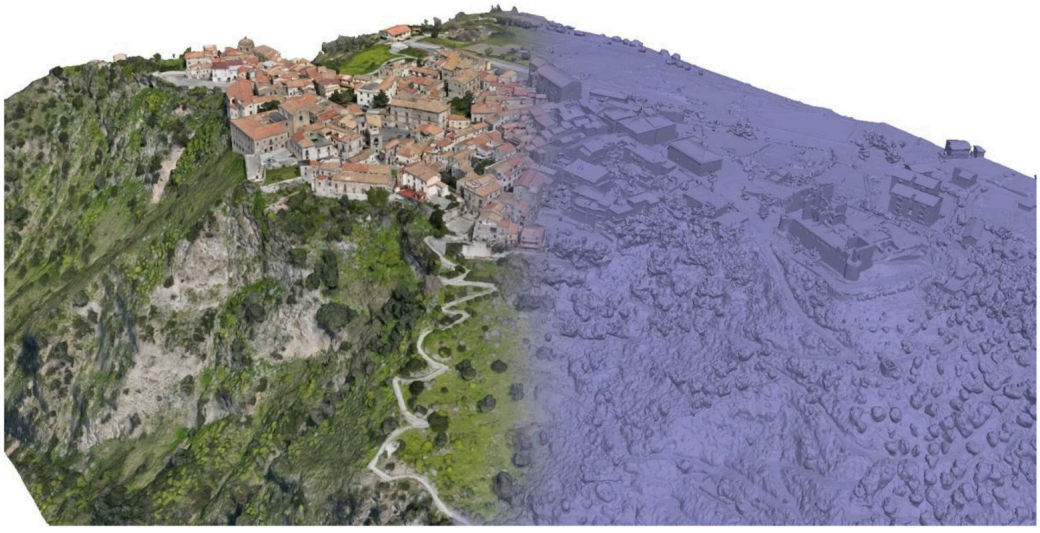


Figure 8. Textured reality-based mesh of Fiumefreddo Bruzio.

3.2. Building-Scale Products and Immersive Interface

As described in Sections 2.4–2.7, for the five buildings of greatest interest, the co-registration of data acquired through TLS, terrestrial and UAV photogrammetry, and SLAM made it possible to generate dense multi-source point clouds referenced to the RDN2008/UTM zone 33N coordinate system. From these datasets, orthophotos of the

main façades and internal architectural surfaces were produced through projection and surface development, including those documenting the painted decorations of Castello della Valle. Vector drawings, including plans, elevations, and sections, were also produced at a nominal scale of 1:50 (Figure 9).



Figure 9. Unfolded orthophotos of the façades of the Church of San Rocco.

The CAD (Computer-Aided Design) documentation was developed on horizontal and vertical planes defined from the point clouds, allowing the representation of room layouts, wall thicknesses, openings, roof profiles, and decorative elements. The integration of orthophotos and vector drawings made it possible to document both the geometric configuration of the spaces and the material characteristics of the architectural surfaces, providing a rigorous metric and knowledge base for subsequent deterioration analyses and specialist modelling activities.

To further support architectural-scale knowledge, an immersive virtual route was developed as a complementary output to the metric products. The acquired route covers a large part of the main street network of the historic centre, providing a continuous and navigable representation of the urban space. Based on the collected data, a client-side web application was developed, directly accessible through a browser, integrating OpenStreetMap vector cartography with a 360° equirectangular video. The route, reconstructed in a GIS environment and exported in GeoJSON format, is synchronised with the video through timestamp–distance checkpoints, allowing variations in acquisition speed to be compensated for while maintaining correspondence between geographic position and the currently displayed video frame.

A dynamic marker shows the real-time position along the route, while interactive checkpoints provide direct access to specific points of interest. The immersive visualisation is implemented using Three.js and WebGL (Web Graphics Library), projecting the video onto a spherical mesh, while the separate distribution of the frontend and multimedia content across cloud services enables the efficient management of large video files. The system therefore provides an integrated tool for heritage communication and enhancement, complementary to the metric and cartographic products derived from the survey (Figure 10).

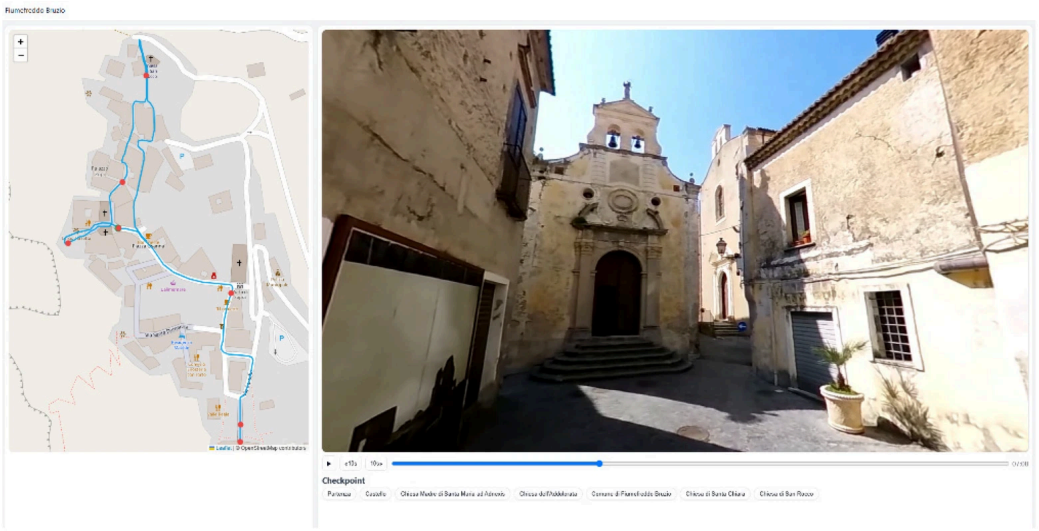
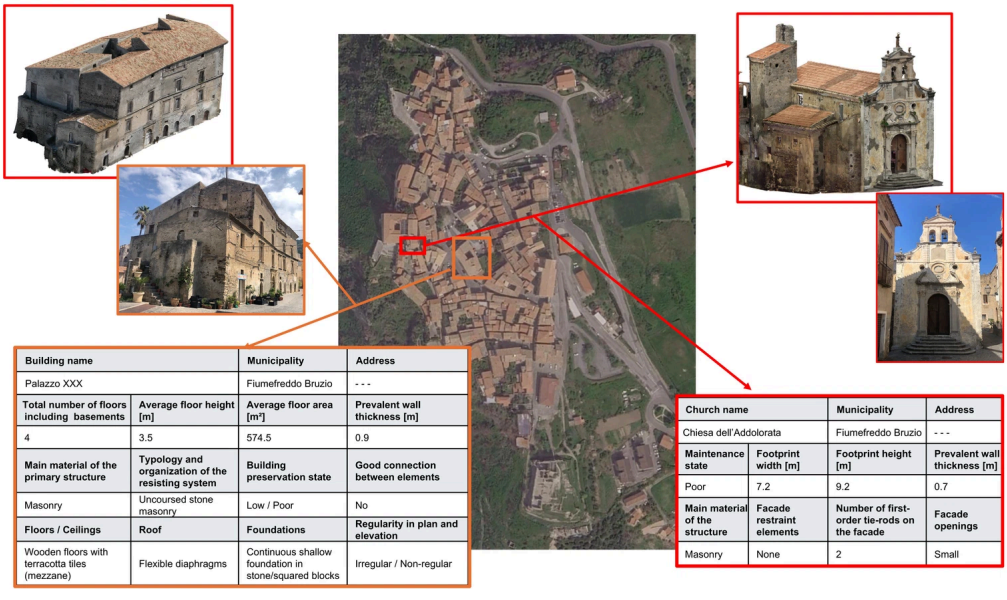


Figure 10. Web interface integrating the route map and 360° video.

3.3. Integrated Information Environment for Multi-Scale Vulnerability

The structural component provides a concrete example of how the geospatial database can provide the basis for developing an updatable information environment. Within the GIS environment, the geometry of each building can be linked to general building information records, descriptions of the structural and construction characteristics relevant to vulnerability assessment, and the preliminary identification of building portions (e.g., façades, macro-elements) potentially susceptible to local kinematic mechanisms during an earthquake. Figure 11 shows an example of the spatial integration of structural data supporting the geospatial digital twin foundation for the Fiumefreddo centre.



Building name		Municipality	Address
Palazzo XXX		Fiumefreddo Bruzio	- - -
Total number of floors including basements	**Average floor height [m]**	**Average floor area [m²]**	**Prevalent wall thickness [m]**
4	3.5	574.5	0.9
Main material of the primary structure	**Typology and organization of the resisting system**	**Building preservation state**	**Good connection between elements**
Masonry	Uncoursed stone masonry	Low / Poor	No
Floors / Ceilings	**Roof**	**Foundations**	**Regularity in plan and elevation**
Wooden floors with terracotta tiles (mezzane)	Flexible diaphragms	Continuous shallow foundation in stone/squared blocks	Irregular / Non-regular

Church name		Municipality	Address
Chiesa dell'Addolorata		Fiumefreddo Bruzio	- - -
Maintenance state	**Footprint width [m]**	**Footprint height [m]**	**Prevalent wall thickness [m]**
Poor	7.2	9.2	0.7
Main material of the structure	**Facade restraint elements**	**Number of first-order tie-rods on the facade**	**Facade openings**
Masonry	None	2	Small

Figure 11. Overview of the integrated information environment for vulnerability assessment.

Starting from the information obtained from the geomatic survey of the entire historic centre and from the associated building information, a simplified seismic vulnerability assessment was previously carried out in [1]. In particular, information like building's footprint, average wall thickness, opening ratio, average spacing between walls and quality of the structural system combined with masonry mechanical proper-

ties available from literature (e.g., [32]) allowed to determine the building collapse capacity in terms of peak ground acceleration (PGAc) using the quantitative-qualitative approach mentioned in Section 2.9. Starting from the value of PGAc and the georeferenced position of each building, the capacity return period T_r of the seismic action corresponding to the occurrence of PGA at the building site location was evaluated using the QGIS processing plugin mentioned in Section 2.9 Specifically, the return period T_r is computed by means of linear interpolation in log-space of known pairs (T_r, PGA) provided by MPS04.

Figure 12 shows the seismic capacity of approximately 40 masonry buildings, expressed in terms of the estimated return period T_r. The investigated stock includes one- to four-storey buildings, mainly characterized by natural stone masonry and showing no evident seismic strengthening interventions. This map provides the information related to the global seismic behaviour of the buildings. Where appropriate, e.g., where masonry portions or façades susceptible to local collapse mechanisms (i.e., macro-elements) were identified, using the survey results (irregularities, out-of-plumbness and existing crack patterns), the procedure was complemented by linear kinematic analyses of their potential out-of-plane response carried out in accordance with [31–33].

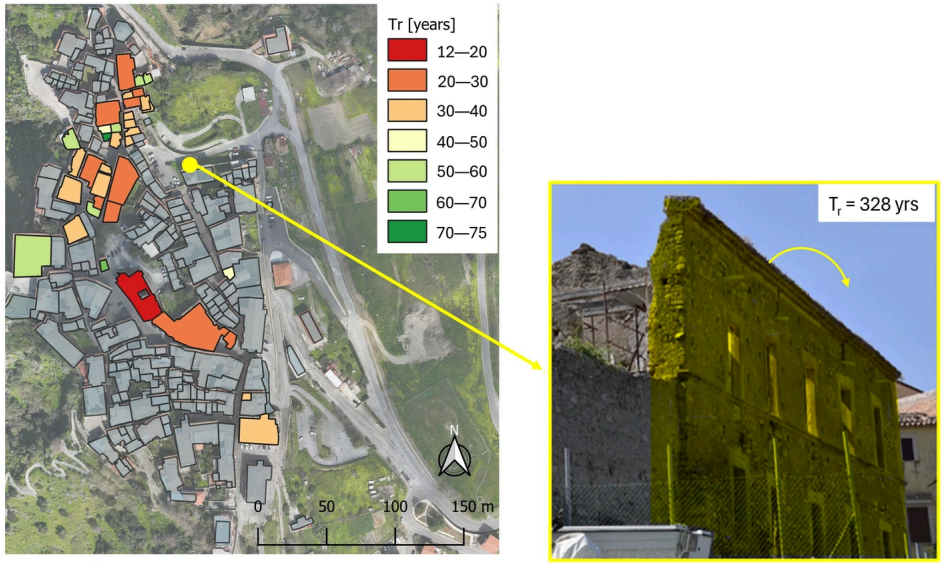


Figure 12. Seismic capacity of a building stock expressed in terms of the return period T_r of the seismic action resisted by each building using screening results previously reported in [1]; example of linear kinematic analysis result for an individuated macro-element.

The castle example demonstrates how high-resolution survey data can be used to identify potentially unstable masonry portions (macroelements) and perform their seismic assessment. Specifically, the three-dimensional model, along with its high-resolution textured mesh, enables the precise detection of wall geometry, structural alignments, openings, and visible crack patterns or discontinuities, which serve as the geometric basis for identifying the macroelements potentially subjected to local collapse mechanisms. Furthermore, the 3D model allows for the exact extraction of geometric parameters, such as the centre-of-gravity coordinates (x_G, z_G) of each macro-element. Figure 13 presents two identified potential collapse mechanisms for the castle and the corresponding re-

sults of the linear kinematic analyses, expressed in terms of return period. In the application of kinematic analysis, PGAc is evaluated dividing the ratio x_G/z_G by the confidence factor FC = 1.35 and adopting the factor q = 2 according to [31,32]. The corresponding return period T_r is obtained using the above mentioned QGIS processing plugin.

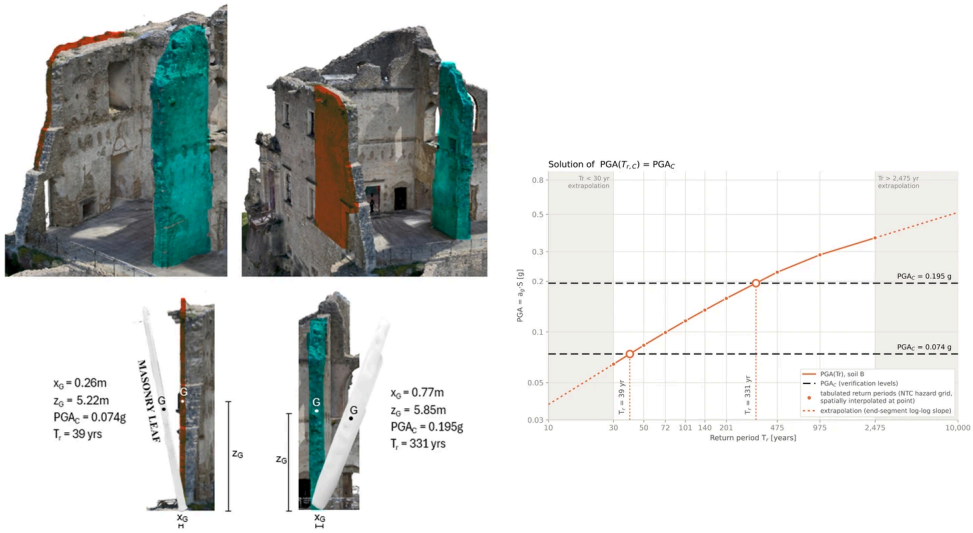


Figure 13. Individuation of possible local collapse mechanisms from the 3D model of the castle with main data and results of the linear kinematic analysis in terms of return period (**left**) and T interpolation (**right**).

The integration within the GIS environment of the seismic vulnerability analysis of entire building as well as of macro-elements is important because the obtained results are no longer isolated value in a calculation sheet: they become queryable properties of a physical asset together with the geomatic survey products, material and structural characteristics, conservation state. Global and local results can coexist in the same architecture, but at different semantic and geometric levels, with explicit links between historic centre, building, façade, macro-element.

3.4. Risk Informed Decision Support/Risk Management and Touristic Valorization

This section describes the potentiality of the framework proposed in integrating vulnerabilities/possible collapses, obstruction of routes and emergency accessibility for risk-management purposes together with touristic valorisation. Within a risk-based approach, the results of the structural assessment could support risk interpretation beyond the scale of the individual building by accounting for the interaction between the built fabric and the surrounding public space. In a compact historic centre even a local or partial collapse may obstruct streets and passages that are essential for ordinary circulation, emergency access and the evacuation of residents and visitors. The structural information could therefore be combined with the street vulnerability and accessibility data already mapped within the geospatial environment, allowing to extend the preliminary approach presented in [1]. This integration could make it possible to relate potentially critical buildings, identified through territorial-scale vulnerability assessment, as well as macro-elements susceptible to local kinematic mechanisms, to the function of adjacent public spaces, thereby identifying situations in which structural damage could compromise strategic routes.

The resulting framework would provide a basis for developing seismic scenarios in

which the consequences of potential collapses are transferred to the street network. Rather than considering only the capacity of individual buildings, these scenarios can highlight possible obstructions, interruptions and changes in accessibility, thus helping to identify priority areas for further investigation or mitigation. The framework may also support the comparison of alternative intervention strategies by considering both the reduction in structural vulnerability and their effects on the overall functioning of the historic centre.

This information could assist decision-making at different stages of seismic risk management. Before an earthquake, it can guide detailed investigations and preventive interventions towards buildings or masonry portions whose failure would have the greatest consequences for emergency access and circulation. Following an event, the pre-existing information could provide a reference for organizing inspections, recording observed damage and rapidly reassessing the usability of streets and buildings. Subsequent strengthening or stabilization measures could then be documented and evaluated in relation to the vulnerability initially identified and to the conservation requirements of the historic fabric.

As an example, Figure 14 illustrates a possible use of the detailed 3D model. The model used for assessment of local collapse mechanism affecting a portion of the castle (Figure 13) was exploited also for the preliminary conceptual design phase of a stabilization solution designed to integrate structural, conservation, functional, and accessibility requirements.



Figure 14. Hypotheses of retrofit interventions of the castle: steel flooring system for connection and internal walkways, designed by Prof. Eng. Arch. Paolo Faccio.

Finally, the three-dimensional reconstruction, combined with the structural stabilization measures, may enable new forms of cultural interpretation and visitor engagement. For the case study, this potential is particularly relevant to the castle, whose exterior once featured frescoes by the renowned Italian artist Salvatore Fiume that have progressively deteriorated due to prolonged exposure to weathering. The geometric and visual information collected through the integrated survey could support the video mapping projection of the frescoes (Figure 15).



Figure 15. Proposed video mapping projection: digital reconstruction of the original Salvatore Fiume's frescoes for site valorization.

Such an application would provide visitors with an immersive interpretation of a partially lost artistic heritage without requiring direct intervention on the surviving fabric. In this way, structural risk mitigation, digital documentation and cultural valorization can operate within a single framework, improving the safe accessibility of the site while supporting the communication and appreciation of its historical and artistic significance.

4. Discussion: From Geometric Information to Structural and Seismic Risk Interpretation

The relevance of the proposed multi-scale framework extends beyond geometric documentation, as the same survey-derived information can support structural interpretation at different spatial levels.

The activities carried out in Fiumefreddo Bruzio highlight how the construction of a coherent information framework requires a multi-sensor strategy tailored to the urban morphology and to the specific objectives of the survey. In a historic mountain settlement, terrestrial and UAV photogrammetry, SLAM, TLS, and GNSS provide complementary capabilities and, when properly integrated, make it possible to mitigate critical issues related to occlusions, confined spaces, trajectory drift, and positioning constraints. The overall reliability of the system therefore depends not only on the nominal specifications of the individual sensors, but also on the geometry of the acquisition network, the operating conditions, the calibration procedures, the adoption of a common reference system, and the availability of independent control procedures.

The quantitative results (Tables 1, 2 and 4) provide evidence of the metric performance of the proposed multi-sensor workflow. The UAV photogrammetric block achieved a reported three-dimensional residual of 0.037 m on 8 independent check points, compared with 0.026 m on the 20 ground control points used for orientation. These results support the metric reliability of the photogrammetric dataset for the intended urban-scale documentation.

The six SLAM acquisitions showed mean planimetric residuals ranging from 0.024 to 0.035 m and mean vertical residuals ranging from 0.031 to 0.049 m at the surveyed control points. These values confirm the suitability of SLAM for connecting different portions of the historic urban fabric, while also highlighting the need to distinguish its

metric performance from that of the other surveying techniques.

At the architectural scale, 270 terrestrial laser scanning stations were acquired across five heritage buildings, providing detailed geometric documentation for the production of plans, elevations, and sections at a nominal scale of 1:50.

These results demonstrate the ability of the adopted workflow to combine datasets characterised by different spatial resolutions and metric performances within a common geodetic reference system. However, the reported residuals should be interpreted according to the validation procedures adopted for each technique, rather than as a uniform accuracy estimate for the complete integrated model.

Regarding the impact of these spatial geometric uncertainties on the overall seismic vulnerability assessment, it is worth noting that their effect is practically negligible compared to other sources of uncertainty in the structural analysis, e.g., mechanical properties of historic masonry, boundary conditions, wall-to-wall and floor-to-wall connection efficiency, together with the seismic action itself, including local site response due to soil characteristics.

At the building scale, the availability of detailed and metrically consistent geometry provides a basis for characterizing structural configuration and for refining the assumptions adopted in seismic assessment. At a higher level of detail, the three-dimensional representation can support the identification and analysis of potentially vulnerable portions of the structure, particularly where local mechanisms may influence the seismic response.

This aspect is particularly relevant for historic masonry, where structural interpretation is often affected by incomplete knowledge and by the complexity resulting from construction phases, transformations and interactions between adjacent units. Increasing geometric resolution does not remove these uncertainties, nor does it replace the engineering assumptions required by structural models, as mentioned above. It does, however, make such assumptions more transparent and verifiable by providing a common spatial reference for observations and structural results. The proposed architecture therefore preserves the distinction between measured data and structural interpretation, while allowing both to evolve within the same information environment.

A further implication concerns the transition from building-scale vulnerability to seismic risk at the scale of the historic centre. In a compact urban fabric such as Fiumefreddo Bruzio, the consequences of structural damage are not necessarily confined to the affected building, since local or partial collapses may interfere with the surrounding public space and alter accessibility during an emergency. Relating structural assessment to the street network therefore provides a means of interpreting vulnerability in spatial terms and of identifying critical interactions between the built fabric and the routes required for evacuation or emergency access. The preliminary analyses presented in [1] provide a first basis for this integration, which can be further developed through revised structural assessments and scenario-based representations at the urban scale.

The main value of the proposed geospatial framework lies in maintaining explicit relationships between measured geometry, structural assessments, and their spatial consequences. This information structure can support the progressive revision of seismic vulnerability and risk scenarios through repeated surveys and post-event observations, while preserving the traceability of the original data and subsequent interpretations.

5. Conclusions

This study presents a multi-sensor and multi-scale geomatics workflow for the documentation and spatial interpretation of the historic centre of Fiumefreddo Bruzio. The integration of UAV and terrestrial photogrammetry, SLAM, TLS and GNSS observations

enabled the construction of a georeferenced geometric information base connecting the urban fabric with the detailed architectural documentation of five selected heritage buildings. The adoption of a common geodetic reference system ensured spatial consistency among datasets acquired at different scales, while the complementary characteristics of the surveying techniques allowed the complex morphology of the settlement to be documented.

The main scientific contribution of this research lies not in the combined use of established surveying technologies, but in the development of a metrically controlled, multi-scale geomatics framework that extends beyond the production of three-dimensional representations. The integration of datasets acquired with different techniques, resolutions, and metric performances provides a common spatial reference while preserving their geometric characteristics, metric quality, and data provenance. This approach establishes a coherent information base in which measured geometry can be related to architectural and structural information without losing the distinction between direct observations and subsequent interpretations.

The integration of geometric information with structural and seismic vulnerability assessments further demonstrates the potential of this approach. At the building scale, detailed survey data support the geometric characterisation of masonry structures and the identification of architectural elements relevant to global and local seismic behaviour. At the urban scale, the geospatial framework allows vulnerability information to be related to the surrounding built environment and street network, supporting the spatial interpretation of potential structural damage and its consequences for accessibility and emergency management. In this way, the proposed methodology establishes a connection between architectural documentation, structural interpretation, and risk-informed conservation strategies.

At its current stage, the proposed system represents a survey-based digital model that can support future HBIM and digital twin developments. Future developments will therefore focus on extending the proposed geometric and information framework through parametric modelling, multi-temporal surveys, change detection, and the updating of structural and seismic risk assessments. Particular attention should also be given to the evaluation of uncertainty in the integration of heterogeneous datasets, ensuring that the metric quality and provenance of the original observations remain accessible throughout subsequent modelling processes.

Author Contributions: Conceptualization, C.B.; methodology, E.B., A.M., L.B. and D.A.T.; software D.A.T.; validation, E.B. and A.M.; data curation, E.B., A.M., L.B., D.A.T. and I.R.; writing—original draft preparation, C.B., E.B., A.M., L.B. and D.A.T.; writing—review and editing, C.B., E.B., A.M., L.B. and D.A.T.; supervision, C.B.; funding acquisition, D.A.T. All authors have read and agreed to the published version of the manuscript.

Funding: This study was funded by the 2025 Iuav University Call project, "Valorisation, Safety and Conservation of Italian Historic Villages and Historic Centres: A Multi-hazard and Multi-scale Approach", of the Università Iuav di Venezia.

Institutional Review Board Statement: Not applicable.

Informed Consent Statement: Not applicable.

Data Availability Statement: At the time of submission, the project data had not been deposited in a public repository. Selected derived datasets may be made available by the corresponding author upon reasonable request, subject to the relevant project, property-owner, and municipal-authority permissions.

Acknowledgments: The authors gratefully acknowledge all contributors to the research activities carried out within the GENESIS project, whose support was essential to the results presented in this study. Furthermore, the authors thank the local authorities and stakeholders who facilitated access to the buildings and survey areas in Fiumefreddo Bruzio. During the preparation of this manuscript, the authors used OpenAI Codex to assist with language editing and the preparation and layout of schematic figures. The authors reviewed and edited all outputs and take full responsibility for the content of the publication.

Conflicts of Interest: The authors declare no conflicts of interest.

Abbreviations

The following abbreviations are used in this manuscript:

CAD	Computer-Aided Design
CP	Check Point
DSM	Digital Surface Model
DTM	Digital Terrain Model
EPSG	European Petroleum Survey Group
GCP	Ground Control Point
GIS	Geographic Information System
GNSS	Global Navigation Satellite System
GSD	Ground Sampling Distance
HBIM	Historic Building Information Modelling
IGM	Italian Military Geographic Institute
NRTK	Network Real-time Kinematic Positioning
PGAc	Peak Ground Acceleration at Collapse
RDN2008	Rete Dinamica Nazionale 2008
RGB	Red, Green, Blue
RMSE	Root Mean Square Error
SfM	Structure from Motion
SLAM	Simultaneous Localisation and Mapping
TLS	Terrestrial Laser Scanning
UAV	Unmanned Aerial Vehicle
UTM	Universal Transverse Mercator
WebGL	Web Graphics Library

References

1. Balletti, C.; Berto, L.; Breggion, E.; Faccio, P.; Guerra, F.; Martinelli, G.D.; Rocca, I.; Saetta, A.; Talledo, D. An Interpretative Model for Seismic Risk: The Case of Fiumefreddo Bruzio in Southern Italy. *Procedia Struct. Integr.* **2026**, *78*, 1823–1830. [Google Scholar] [CrossRef]
2. Kritzinger, W.; Karner, M.; Traar, G.; Henjes, J.; Sihn, W. Digital Twin in Manufacturing: A Categorical Literature Review and Classification. *IFAC-PapersOnLine* **2018**, *51*, 1016–1022. [Google Scholar] [CrossRef]
3. Boje, C.; Guerriero, A.; Kubicki, S.; Rezgui, Y. Towards a Semantic Construction Digital Twin: Directions for Future Research. *Autom. Constr.* **2020**, *114*, 103179. [Google Scholar] [CrossRef]
4. Sacks, R.; Brilakis, I.; Pikas, E.; Xie, H.S.; Girolami, M. Construction with Digital Twin Information Systems. *Data-Centric Eng.* **2020**, *1*, e14. [Google Scholar] [CrossRef]
5. Jouan, P.; Hallot, P. Digital twin: A HBIM-based methodology to support preventive conservation of historic assets through heritage significance awareness. *Int. Arch. Photogramm. Remote Sens. Spat. Inf. Sci.* **2019**, *XLII-2/W15*, 609–615. [Google Scholar] [CrossRef]

6. Liu, Z.; Wang, J. Protection and Utilization of Historical Sites Using Digital Twins. *Buildings* **2024**, *14*, 1019. [Google Scholar] [CrossRef]
7. Vuoto, A.; Funari, M.F.; Lourenço, P.B. On the Use of the Digital Twin Concept for the Structural Integrity Protection of Architectural Heritage. *Infrastructures* **2023**, *8*, 86. [Google Scholar] [CrossRef]
8. Sivori, D.; Ierimonti, L.; Venanzi, I.; Ubertini, F.; Cattari, S. An Equivalent Frame Digital Twin for the Seismic Monitoring of Historic Structures: A Case Study on the Consoli Palace in Gubbio, Italy. *Buildings* **2023**, *13*, 1840. [Google Scholar] [CrossRef]
9. Spanò, A.; Patrucco, G.; Sammartano, G.; Perri, S.; Avena, M.; Fillia, E.; Milan, S. Digital Twinning for 20th Century Concrete Heritage: HBIM Cognitive Model for Torino Esposizioni Halls. *Sensors* **2023**, *23*, 4791. [Google Scholar] [CrossRef] [PubMed]
10. Murphy, M.; McGovern, E.; Pavia, S. Historic Building Information Modelling—Adding Intelligence to Laser and Image Based Surveys of European Classical Architecture. *ISPRS J. Photogramm. Remote Sens.* **2013**, *76*, 89–102. [Google Scholar] [CrossRef]
11. Dore, C.; Murphy, M. CURRENT STATE OF THE ART HISTORIC BUILDING INFORMATION MODELLING. *Int. Arch. Photogramm. Remote Sens. Spat. Inf. Sci.* **2017**, *XLII-2/W5*, 185–192. [Google Scholar] [CrossRef]
12. López, F.J.; Lerones, P.M.; Llamas, J.; Gómez-García-Bermejo, J.; Zalama, E. A Review of Heritage Building Information Modeling (H-BIM). *Multimodal Technol. Interact.* **2018**, *2*, 21. [Google Scholar] [CrossRef]
13. Matrone, F.; Colucci, E.; De Ruvo, V.; Lingua, A.; Spanò, A. HBIM IN A SEMANTIC 3D GIS DATABASE. *Int. Arch. Photogramm. Remote Sens. Spat. Inf. Sci.* **2019**, *XLII-2/W11*, 857–865. [Google Scholar] [CrossRef]
14. Sammartano, G.; Avena, M.; Fillia, E.; Spanò, A. Integrated HBIM-GIS Models for Multi-Scale Seismic Vulnerability Assessment of Historical Buildings. *Remote Sens.* **2023**, *15*, 833. [Google Scholar] [CrossRef]
15. Kutzner, T.; Chaturvedi, K.; Kolbe, T.H. CityGML 3.0: New Functions Open up New Applications. *PFG–J. Photogramm. Remote Sens. Geoinf. Sci.* **2020**, *88*, 43–61. [Google Scholar] [CrossRef]
16. Ledoux, H.; Arroyo Ohori, K.; Kumar, K.; Dukai, B.; Labetski, A.; Vitalis, S. CityJSON: A Compact and Easy-to-Use Encoding of the CityGML Data Model. *Open Geospat. Data softw. stand.* **2019**, *4*, 4. [Google Scholar] [CrossRef]
17. Remondino, F.; El-Hakim, S. Image-based 3D Modelling: A Review. *Photogramm. Rec.* **2006**, *21*, 269–291. [Google Scholar] [CrossRef]
18. Nex, F.; Remondino, F. UAV for 3D Mapping Applications: A Review. *Appl. Geomat.* **2014**, *6*, 1–15. [Google Scholar] [CrossRef]
19. James, M.R.; Robson, S.; Smith, M.W. 3-D Uncertainty-based Topographic Change Detection with Structure-from-motion Photogrammetry: Precision Maps for Ground Control and Directly Georeferenced Surveys. *Earth Surf. Process. Landf.* **2017**, *42*, 1769–1788. [Google Scholar] [CrossRef]
20. Sanz-Ablanedo, E.; Chandler, J.H.; Rodríguez-Pérez, J.R.; Ordóñez, C. Accuracy of Unmanned Aerial Vehicle (UAV) and SfM Photogrammetry Survey as a Function of the Number and Location of Ground Control Points Used. *Remote Sens.* **2018**, *10*, 1606. [Google Scholar] [CrossRef]
21. Sammartano, G.; Spanò, A. Point Clouds by SLAM-Based Mobile Mapping Systems: Accuracy and Geometric Content Validation in Multisensor Survey and Stand-Alone Acquisition. *Appl. Geomat.* **2018**, *10*, 317–339. [Google Scholar] [CrossRef]
22. Rodríguez-Gonzálvez, P.; Jiménez Fernández-Palacios, B.; Muñoz-Nieto, Á.; Arias-Sanchez, P.; Gonzalez-Aguilera, D. Mobile LiDAR System: New Possibilities for the Documentation and Dissemination of Large Cultural Heritage Sites. *Remote Sens.* **2017**, *9*, 189. [Google Scholar] [CrossRef]
23. Balletti, C.; Breggion, E.; Gerla, F.; Guerra, F.; Martino, A. Venice: A Test Field for Urban Historical Centers Surveying with SLAM. In Proceedings of the 2024 IEEE International Workshop on Metrology for Living Environment (MetroLivEnv), Chania, Greece, 12–14 June 2024; pp. 224–229. [Google Scholar]
24. Mohammadi, M.; Rashidi, M.; Mousavi, V.; Karami, A.; Yu, Y.; Samali, B. Quality Evaluation of Digital Twins Generated Based on UAV Photogrammetry and TLS: Bridge Case Study. *Remote Sens.* **2021**, *13*, 3499. [Google Scholar] [CrossRef]
25. Fascia, R.; Barbieri, F.; Gaspari, F.; Ioli, F.; Pinto, L. From 3D survey to digital reality of a complex architecture: A digital workflow for cultural heritage promotion. *Int. Arch. Photogramm. Remote Sens. Spat. Inf. Sci.* **2024**, *XLVIII-2/W4-2024*, 205–212. [Google Scholar] [CrossRef]
26. Mozas-Calvache, A.T.; Gómez-López, J.M.; Pérez-García, J.L.; Vico-García, D.; Barba-Colmenero, V.; Fernández-Ordóñez, A. Multi-Sensor Geomatic Techniques for the 3D Documentation and Virtual Repositioning of Elements of the Church of S. Miguel (Jaén, Spain). *Heritage* **2024**, *7*, 2924–2943. [Google Scholar] [CrossRef]
27. Istituto Geografico Militare. Elementi Geodetici—La Rete Dinamica Nazionale (RDN). Available online: https://igmi.esercito.difesa.it/descrizione-prodotti/elementi-geodetici/ (accessed on 16 July 2026).

28. FARO Technologies; Inc. Performance Specifications for the Focus3D. Available online: https://knowledge.faro.com/Hardware/Focus/Focus/Performance_Specifications_for_the_Focus3D (accessed on 11 September 2026).
29. Talledo, D.A.; Rocca, I.; Berto, L.; Saetta, A. Application of Hybrid Quantitative-Qualitative Models for Seismic Vulnerability of Historic City Centers. In Proceedings of the 10th International Conference on Computational Methods in Structural Dynamics and Earthquake Engineering (COMPDYN 2025), Rhodes Island, Greece, 15–18 June 2025; pp. 2903–2912. [Google Scholar]
30. Ferretti, F.; Mazzotti, C.; Savoia, M. Seismic Vulnerability Assessment of Masonry and RC Building Stocks: A Simplified Methodology. *Buildings* **2024**, *14*, 2890. [Google Scholar] [CrossRef]
31. Ministero delle Infrastrutture e dei Trasporti. *Decreto 17 Gennaio 2018: Aggiornamento delle Norme Tecniche per le Costruzioni*; Gazzetta Ufficiale della Repubblica Italiana: Rome, Italy, 2018.
32. Ministero delle Infrastrutture e dei Trasporti. *Circolare 21 Gennaio 2019, No. 7 C.S.LL.PP.: Istruzioni per l'Applicazione dell'Aggiornamento delle Norme Tecniche per le Costruzioni*; Gazzetta Ufficiale della Repubblica Italiana: Rome, Italy, 2019.
33. Mori, F.; Mendicelli, A.; Moscatelli, M.; Romagnoli, G.; Peronace, E.; Naso, G. A New Vs30 Map for Italy Based on the Seismic Microzonation Dataset. *Eng. Geol.* **2020**, *275*, 105745. [Google Scholar] [CrossRef]

Disclaimer/Publisher's Note: The statements, opinions and data contained in all publications are solely those of the individual author(s) and contributor(s) and not of MDPI and/or the editor(s). MDPI and/or the editor(s) disclaim responsibility for any injury to people or property resulting from any ideas, methods, instructions or products referred to in the content.